3

Scientific and engineering principles in other texturing processes

3.1 Introduction

Many of the comments in Chapter 2 apply to other methods of texturing. From Section 2.2, the fibre science is the same and most methods involve heat-setting, though in forms different from that in twist-texturing. The one process that has major differences is air-jet texturing, which involves a mechanical locking of loops that project from the yarn. Heat-setting, if applied after texture formation, is a secondary stabilising factor.

3.2 Bending, buckling and setting

3.2.1 Planar crimp

In knit-de-knit texturing (and if gear-crimping was used), the fibres are forced into a planar, or almost planar, wave-like form and heat-set. The bulk and stretch features come from the amplitude and period of the crimp, with subtler differences due to the shape of the waves. Since these processes are applied to yarns, the crimp will tend to be in register in neighbouring filaments. The tension to extend the yarns from the crimped state results from the unbending forces (Section 2.2.8).

3.2.2 Bicomponent bulking

Two methods of producing textured filament yarns depend on producing differences between opposite sides of filaments. Neither are primary concerns of this book, but the principles should be mentioned briefly. In the obsolete *Agilon* process, this was achieved by passing the yarn over a sharp edge, which resulted in a change of fibre structure in the part nearest the edge. In bicomponent-fibre yarns, fibre producers extrude two different components side-by-side. Fibres of these types act like a bimetallic strip and

differential contraction causes them to take up bent forms. The behaviour is that described in Section 2.6.3 and leads to the formation of alternating right- and left-handed helices with reversal regions in between, which can be seen if Fig. 1.1(b) is examined carefully. Figure 3.1 shows the complicated form taken up by a nylon/elastomer bicomponent fibre after break. The high level of differential contraction leads to tight coils.

3.2.3 Stuffer-box and related processes

Another basic technique is to overfeed yarns into a situation where they are forced to take up buckled forms, in which they are heat-set. The distorted forms result from collapse due to mechanical restraint. In the *Ban-Lon* process, which is now obsolete, yarns were forced into a stuffer box and then withdrawn more slowly through a restricted outlet: the input end of the box was hot and the output end was cold. Stuffer-box yarns tend to have an irregular, planar zig-zag form of crimp.

Another method that has been used in the past is the moving-cavity process. Here yarn is blasted on to a screen, where it is fed as a caterpillar through hot and cold zones, in order to set the yarn. The forms taken up here will depend on the way in which yarns buckle as they collapse on the screen. This has not been subject to academic study, but there may be relevance in experimental and theoretical studies of collapse, which were made in the context of laydown of filaments in spun-bonded processes (Hearle *et al*, 1976a,b,c). Figure 3.2(a) illustrates how the form varies with the relative speeds of feed and collector and Fig. 3.2(b) shows a theoretical computation by Konopasek (1980) of the form taken by a fibre as it is fed onto a plane. The mechanics of this analysis was based on force and moment equilibrium along a fibre under given boundary conditions. Methods such as this, or more likely energy-minimisation techniques, would need to be combined with the effect of aerodynamic and solid-contact forces, in order to predict the forms taken by fibres in processes of this type.

3.1 Monvelle, which was a nylon/elastomer bicomponent fibre, after rupture.

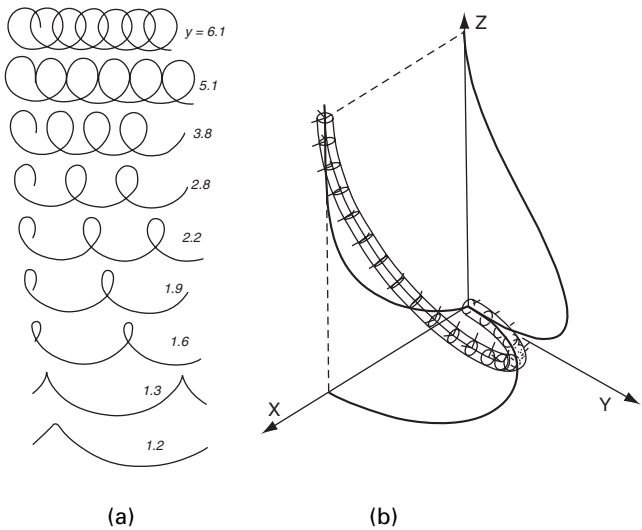

3.2 (a) Predicted forms for collapse of a thread on a moving belt, with decreasing overfeed from top to bottom. From Hearle *et al* (1976b). (b) Computed three-dimensional form during lay-down. From Konopasek (1980).

3.2.4 Hot-fluid texturing

In the jet-screen process used in the production of BCF carpet yarns, yarns are fed through a hot-air or steam jet onto a revolving drum. Although the collapse on the drum may have some influence on the crimped form taken by the fibres, the dominant cause of buckling is the action of the hot jet. The same principle applies to the old *FibreM* process, in which yarn is fed by a hot jet into a tube.

Inevitably, in a turbulent jet, fibres will be heated unevenly. Shrinkage on one side of the fibre will be greater than on the other. Individual segments of filaments will thus act as bicomponent fibres. However, the boundaries between the two sides will change in direction along the fibre. Because of the differential shrinkage, which probably varies in magnitude, the fibre segments will bend into curvatures that minimise energy. However, because of the irregularity, the fibres will crimp into irregular helical sequences. The twist will be compensated for by the tendency of fibres to bend in different directions. The aerodynamic forces may also influence the form of buckling. The developments have been empirical and the behaviour of fibres in jets, which lead to the distorted paths, has not been studied. The movement of fibres under aerodynamic forces is important in many textile processes, and computational approaches are being developed. In the future, these may

lead to predictive engineering design for jet-texturing, which takes account of the differential heat transfer to the fibres.

3.2.5 The value of a reservoir

Despite its limitations in yarn character, the stuffer-box process has one particular advantage. In false-twist texturing, a tightly twisted yarn, which is held straight under tension, has to be heated and cooled. Inevitably, this means long heating and cooling zones. However, in a stuffer-box the speed of the plug of yarn is less than that of the yarn throughput speed by a factor equal to the ratio of plug linear density to yarn linear density. For orders of magnitude of yarn and box diameter of 0.1 and 10 mm, and ignoring differences in packing factor, this ratio would be 10^4 times. Consequently, in principle, high throughput speeds could be combined with reasonable dimensions of hot and cold zones. The box acts as a reservoir for the heating and cooling operation. In practice, high-speed winders were not available when the stuffer-box process was current.

The caterpillar in jet-screen texturing and the tube in *FibreM* also act as reservoirs for cooling, which is important to prevent bulk being pulled out. If necessary to give enough set, heat can be applied to the zero-tension bulked yarn at the start of the reservoir. Although the speed ratio for the hot-jet region is not as great as for a stuffer-box, the filaments are following distorted paths, so that the yarn throughput speed is reduced. More important, the filaments are separated and so can be directly heated by the hot fluid. The distance for thermal conduction is reduced by a factor equal to the ratio of fibre diameter to yarn diameter, which roughly equals the square root of the number of filaments. This is one reason why jet-screen bulking is preferred to false-twist texturing for coarse carpet yarns; the other reason is that the ratio of fibre twist angle to yarn twist angle is small in twist texturing of yarns with many filaments.

3.3 Air-jet texturing

3.3.1 Trapping of fibre loops

The principle of air-jet texturing, originally introduced as *Taslan*, is clear. Yarn is overfed into a jet and the excess length of filaments appears as projecting loops. In the original process, the yarn was twisted on take-up, in order to lock in the loops. Although much of the development of jets has been empirical, two principles have become clear in later advances. First, the yarn should make a right-angled bend as it emerges from the jet. This is the point at which the loops are forced out of the main body of the yarn.

Second, interlacing of filaments in the jet can cause the loops to be locked into the yarn, so that twist is unnecessary. If two yarns are fed in, the one with lower overfeed will be more important for the core and the one with higher overfeed will be more important for the loops.

Differences in jet-design and process conditions lead to different patterns of loop formation. In addition to the practical experience of commercial manufacturers, there have been academic studies of the action of jets (Acar and Wray 1986a,b; Acar *et al* 1986a–e), which consider the air-flows and the forces acting on the fibres. Other studies have observed yarn forms and how they depend on process parameters (Kollu 1982, 1985; Demir 1987). Some of these studies have used yarns with dyed tracer fibres. When these are viewed microscopically with immersion in a liquid of similar refractive index to the fibres, they show the interlacing of fibre paths within the core of the yarn.

Acar *et al* (1986e) postulate the following mechanism of loop formation. Owing to differences in air-drag forces, some fibres will be moving faster than others. They will slip past slower moving fibres and, at the right-angle bend, be forced forward as loops. The leading ends will be trapped in the interlaced core and will move forward at the relatively slower speed of yarn take-up, whereas the trailing ends will be blown at high speed by the air-jet. Figure 3.3 is a schematic illustration of the sequence. In Fig. 3.3(a) loops L3–L5 have already been formed and trapped, and filaments 1–3 have been pulled forward by the air-stream. Eventually, trailing ends become trapped and loops L1 and L2 form (Fig. 3.3(b,c)). However, the point of loop formation depends on the degree of freedom of the filaments. Consequently, filament 3 is still moving out in Fig. 3.3(c), but filament 4 has been trapped as L4 ahead of L2 (Fig. 3.3(b,c)).

Figure 3.4 shows a typical yarn with many filaments. The various forms of loops have been categorised by Kollu (1982), as shown in Fig. 3.5. Any representative length of yarn can be characterised by a core diameter and

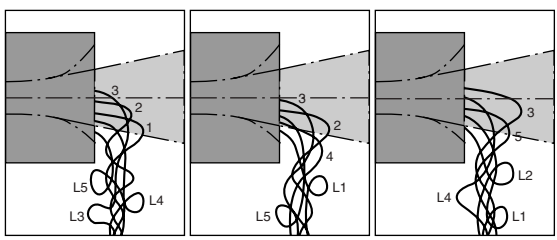

3.3 Schematic illustration of loop formation with five filaments. From Acar *et al* (1986e).

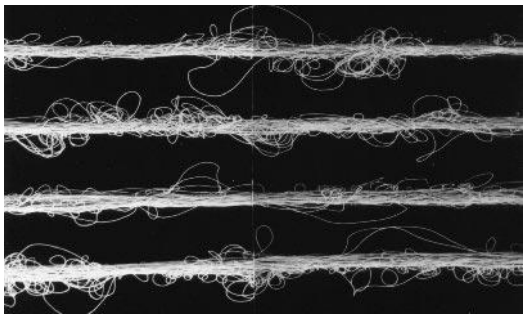

3.4 Polyester air-jet textured yarn with dual overfeeds of 25% and 33%. From Kollu (1982).

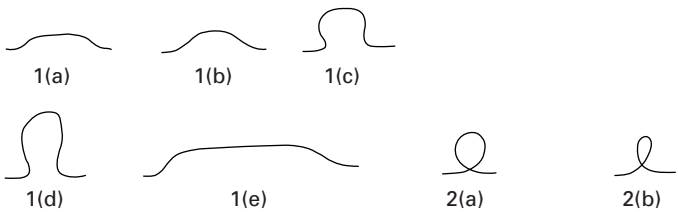

3.5 Categories of loops. From Kollu (1982).

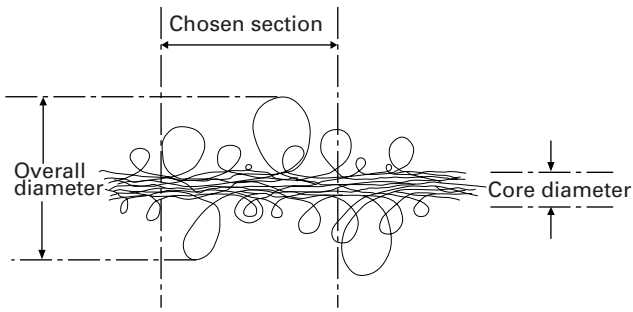

3.6 Characterisation of yarn diameter. From Kollu (1982).

an overall diameter, as shown in Fig. 3.6. A more detailed analysis can be made by scanning an image, such as Fig. 3.7(a), with a microdensitometer to give the plots in Fig. 3.7(b). At the core of the yarn, most of the signal is high, indicating the presence of white fibres, but there are occasional low values where fibre is missing from the image. At 0.44 mm out from the centre, the peaks indicate loops and the low levels indicate their absence. At 0.66 mm out, there are fewer loops and at 0.88 mm there are none.

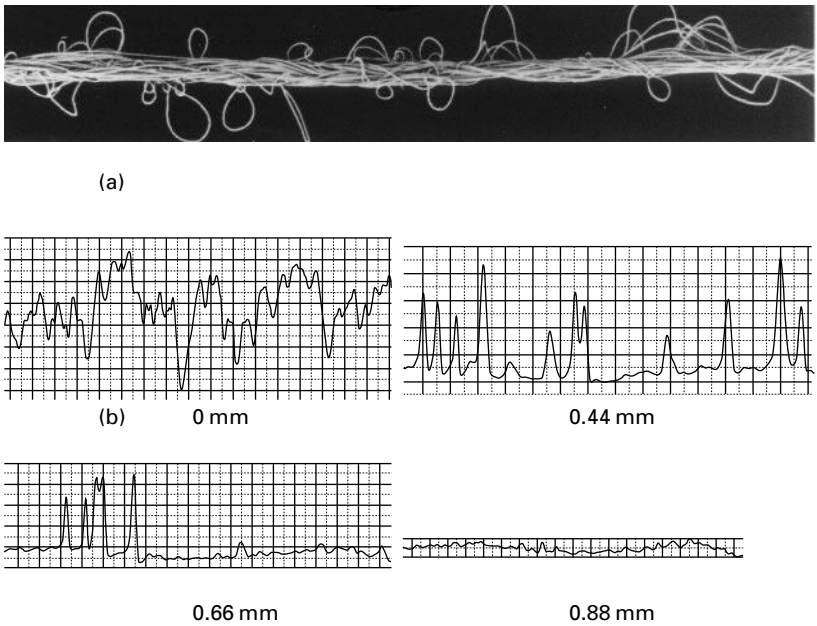

3.7 (a) Air-textured yarn. (b) Microdensitometer scans at distances shown from yarn centre. From Kollu (1982).

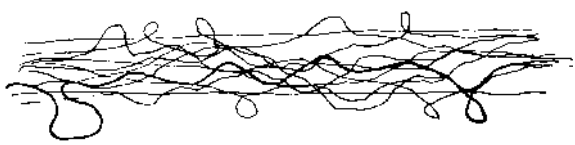

3.8 Schematic illustration of yarn structure. From Kollu (1985).

3.3.2 Yarn geometry

Figure 3.8 is a schematic illustration of the yarn structure. The total yarn linear density, C_y, can be regarded as being made up of two parts, the main core of the yarn, $C_{y,c}$, and the loops, $C_{y,l}$. The bulk of the yarn is determined by the effective radius round the loops, though in fabrics, this will depend on the extent to which the loops are squashed by the neighbouring yarns. The packing factor in the core can also be low, especially with mixed yarns.

Within the core, the fibres are interlaced. One structural feature consists of the angles θ which fibre elements make to the yarn axis. The other feature, the nature of the interlacing, is less easy to characterise. Kollu (1985), in a mechanical analysis, represented it by a collection of interconnected helices (Fig. 3.9).

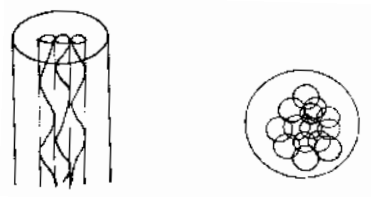

3.9 Schematic indication of fibres in core as overlapping helices. From Kollu (1985).

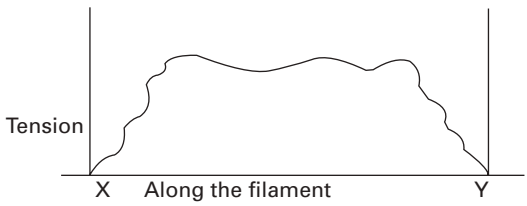

3.10 Tension along a fibre from X to Y in Fig. 3.11. From Kollu (1985).

3.3.3 Yarn tensile properties

A critical question for air-jet textured yarns is whether the loops are locked into the yarn or whether they are pulled out when tension is applied. This is related to the prediction of the tensile stress–strain response of the yarns. Both the uncertainty about the structural details and the difficulties of modelling the complexities mean that no exact analysis has been carried out. However, the approximate treatment that follows brings out the important principles. The analysis follows the treatment of the mechanics of spun-staple yarns (Hearle *et al*, 1969). The projecting loops act in the same way as free fibre ends. The only differences are that the loops occur only at the surface of the core yarn, whereas fibre ends may be outside or inside staple yarns – and that, if there is complete slippage, the yarn finally acts as a strong, continuous-filament yarn instead of breaking. The essential similarity is that the tension is zero in both fibre ends and loops and builds up as the fibres are gripped within the yarns, as illustrated in Fig. 3.10. In predicting the yarn stress at a yarn extension, e, we start with the fibre stress, f_f, at the same strain, and then see how this is reduced in the yarn. In the approximate analysis given here, the same equations apply to the relationship of yarn strength to fibre strength, when yarn breakage results from fibre breakage.

First, we take out the fibre mass in the loops, since these will not contribute to yarn tension. This introduces the factor $(C_{y,c}/C_y)$. Next, we take account of the obliquity of the fibres in the core of the yarn, which reduces

both the fibre strain and the axial component of tension. Approximately, this is given by the mean value $\overline{\cos^4\theta}$. Then we have to allow for slip from the ends of the loops, given by a slip factor *SF*. This gives the yarn stress as (fibre stress at same strain × non-contributing factor × obliquity factor × slip factor):

$$f_y = f_f \times (C_{y,c}/C_y) \times \overline{\cos^4\theta} \times SF \qquad [3.1]$$

The slippage is the factor of most interest. If we consider a fibre, as shown in Fig. 3.11, slip will start from the points X and Y, where the fibre comes out into loops. At these points the fibre tension is zero. Within the core yarn, the fibre is gripped by transverse forces from neighbouring fibres as indicated in Fig. 3.12, and consequently there will be a frictional resistance to slip. The tension will build up as indicated in Fig. 3.13 until it reaches the value $f_f \overline{\cos^4\theta}$ determined by yarn extension and fibre obliquity in the central, fully gripped region. If the length over which slip takes place is *S* and the length between loops is *L*, there is a loss of a fraction *S*/*L* compared to the tension without slip. Hence:

$$SF = 1 - S/L \qquad [3.2]$$

The slip length is given by equating the tensions at the junction of the slip and gripped zones. The resistance to slip is given by the frictional force acting on an area equal to the fibre circumference, $2\pi a$, where *a* is the fibre

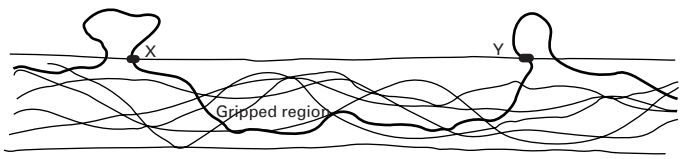

3.11 Fibre between loops in yarn.

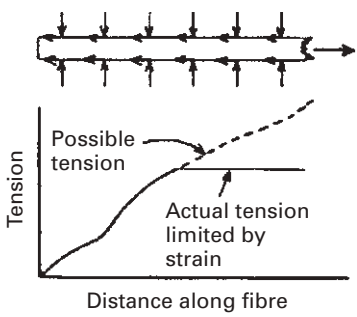

3.12 Build-up of tension due to friction. From Hearle *et al* (1969).

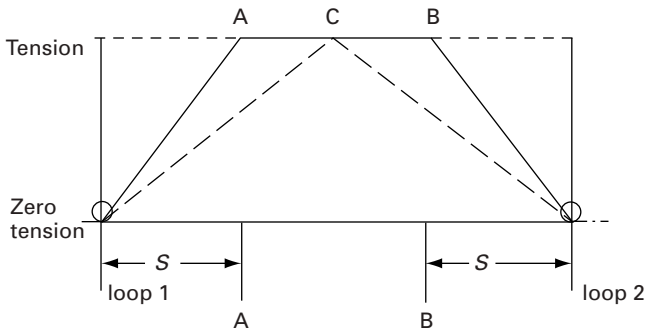

3.13 Linearised indication of tension variation along a fibre between loops. From Kollu (1985).

radius. The frictional shear stress is given by the coefficient of friction, μ, multiplied by the transverse stress from the neighbouring fibres. Roughly, this can be put equal to $\mathcal{F}f_y$, where $\mathcal{F}$ is an operational factor that determines how the yarn tension is converted into transverse forces within the entangled core. The tensile stress in the gripped region is put equal to the fibre area multiplied by the yarn stress. Hence, we obtain the following equations and can substitute for S in equation [3.2]:

$$(2\pi a)S\mu\mathcal{F}f_y = (\pi a^2)f_y \qquad [3.3]$$

and

$$SF = 1 - \tfrac{1}{2}(a/\mu\mathcal{F}L) \qquad [3.4]$$

The factors which minimise slip are thus fine fibres, long lengths between loops, high friction and high conversion of tensile stress into transverse stress between fibres. The form of equation [3.4] is shown in Fig. 3.14. However, a critical situation is reached when $SF = \frac{1}{2}$. At this point, the two slip lines in Fig. 3.13 would meet at the grip tension, so that the fibre would no longer be gripped anywhere. In spun yarns, where the transverse forces result from yarn twist, this corresponds to the boundary between self-locking yarns and draftable rovings. On the simplest argument, the tension would drop to zero; in practice there will be a low frictional resistance to slip. In order to prevent slippage of loops, it is therefore necessary that $(\mu\mathcal{F}L/a) > 1$.

The discerning reader will pick up various inaccuracies in the above argument. Some of these can be corrected by more detailed analysis, which brings in numerical factors, powers and correction terms. However, the general form of the dependence of resistance to slip on μ, $\mathcal{F}$, L and a is valid. The problem which remains is what determines the operational factor, $\mathcal{F}$. How is yarn tension converted into transverse gripping forces? As shown in Fig. 3.15(a,b), it is not fibre orientation that leads to transverse forces,

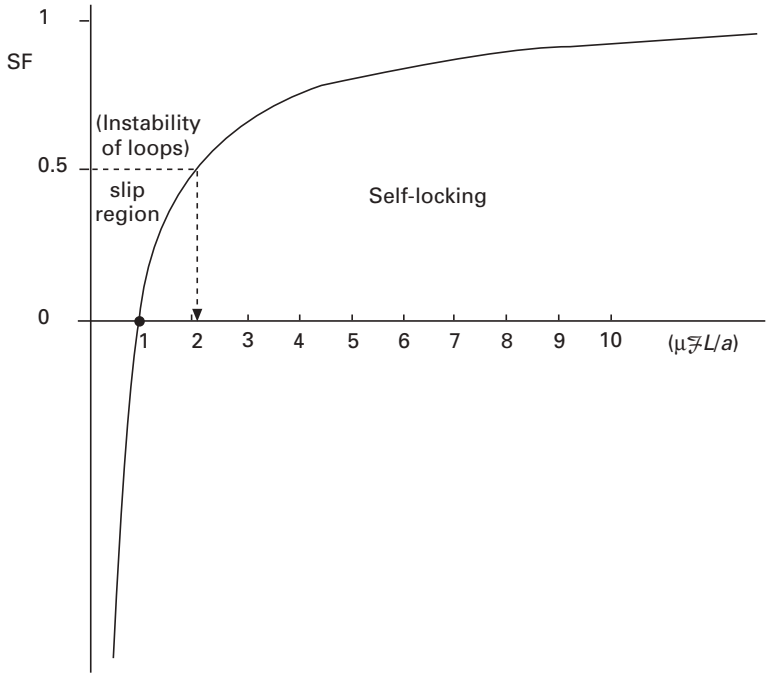

3.14 Form of equation [3.4] for slip factor plotted against ($\mu \mp L/a$). From Kollu (1985).

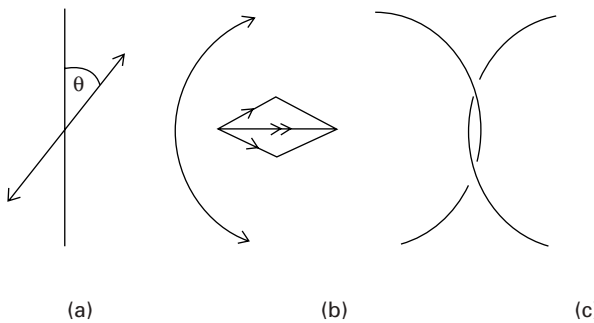

3.15 (a) Tension in a straight fibre at angle θ does not generate transverse forces. (b) Resultant normal force from tension in a curved fibre. (c) Interlocking fibres.

but change of orientation along fibres. Where fibres are following a curved path, as in Fig. 3.15(b), a component of tension acts at right angles to the fibre axis. Consequently, if two fibres are interlaced, as in Fig. 3.15(c), there will be a gripping force between them. This sort of local interaction may

play a part in the core of air-jet textured yarns. However, it is more likely that groups of fibre will be wrapping round each other, so that there is a build-up from outer layers to inner layers. In simple twisted yarns, with successive helical layers, this build-up can be calculated. It is more difficult to see how to deal with the problem in an irregularly interlaced core.

Kollu (1985) adopted the model of interlacing helices, shown in Fig. 3.9. In order to make analysis possible, filaments with a linear density, C_f, are assumed to follow regular helices, with a radius, r, and a helix angle, θ, which will equal the orientation angle of filaments in the yarn. Assuming that n helices surround a fibre and that a fraction, F, of them are 'effective', Kollu calculated the transverse stress acting on the fibre. His equation is equivalent to:

$$\mathcal{F} = F(nC_f)\sin^2\theta/2\pi r^2 \qquad [3.5]$$

Considering the factors in turn, the notion of effective helices involves a technical, statistical effect. If, as in Fig. 3.16, we consider a fibre AB with surrounding helices, the transverse forces from the helices shown as full lines will contribute to the transverse pressure on X, but those shown dotted will oppose the build-up of transverse pressure. The parameters, n and C_f, are interrelated: if the fibres are larger, there will be fewer of them. The helix parameters, r and θ, are 'average' values. Any short, curved segment of fibre in the core of the yarn can be regarded as part of a helix with particular values of radius and angle. Average values could thus be calculated, if the fibre paths are known, though these are not easy to determine.

Kollu (1985), after considering models which indicate values of the effectiveness factor, F, and the interaction of geometrical factors, found a

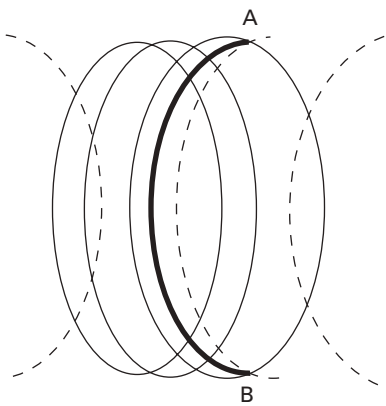

3.16 Portions of overlapping helices.

slippage factor for a yarn of radius, R. Noting that in this model the orientation angle is taken to be constant, this converts equation [3.1] into:

$$f_y = f_f \times (C_{y,c}/C_y) \times \overline{\cos^4\theta} \times \left[1 - K(a/\mu L)(r/R)^m \operatorname{cosec}^2\theta\right] \qquad [3.6]$$

where K is a numerical factor, which may depend on the number of filaments in the yarn, and m is a power between 1 and 2. Although there are many approximations and uncertainties in Kollu's analysis, it is likely that the dependence on r/R and θ probably shows the right trend. It is interesting that the dependence on θ has the same form as for spun-staple yarns

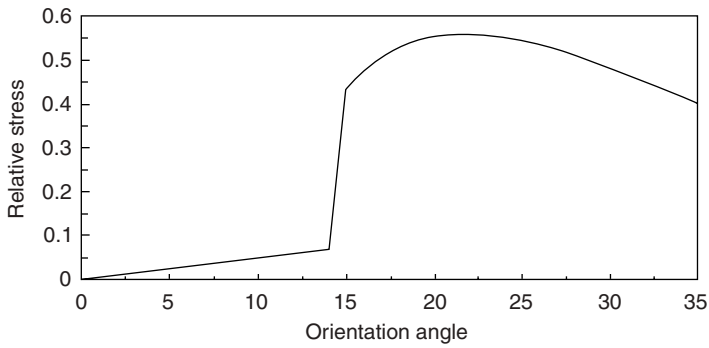

3.17 Dependence of yarn tensile properties as a fraction of fibre properties on helix angle θ.

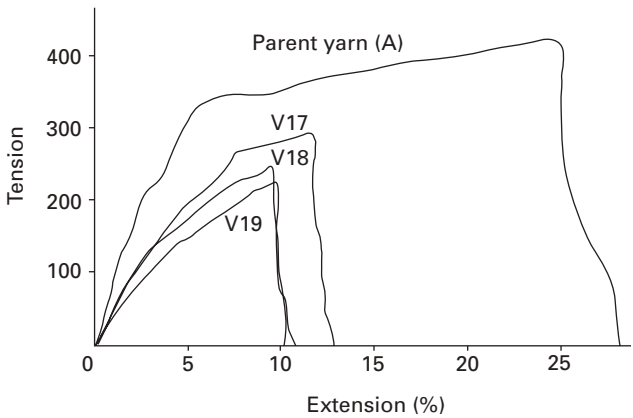

3.18 Load–extension curves for parent yarn and yarn textured at 10% (V17), 15% (V18) and 20% (V19).

(Hearle *et al*, 1969). In practice, this model indicates that, in order to avoid slippage, the jet should provide interlacing in the core of the yarn with a small effective helix radius, though appreciably greater than the fibre radius, and a high helix angle, which gives a low value of $\text{cosec}^2\theta$. Figure 3.17 shows the dependence of f_y, the yarn stress at a given extension, on the orientation angle. Because of the counter-effects of obliquity and slip, there is an optimum degree of interlacing for maximum resistance to extension, and a critical condition for loops to slip. In the gripped region, the curve will also show the trend for strength variation, $f_y = f_y \times (C_{y,c}/C_y) \times \overline{\cos^4\theta} \times SF$. Figure 3.18 shows yarn load–extension curves with tension reducing as overfeed is increased.